Robotica (2012) volume 30, pp. 783–797. © Cambridge University Press 2011
doi:10.1017/S0263574711001032

Multiobjective optimization of parallel kinematic mechanisms by the genetic algorithms

Ridha Kelaiaia†,‡,* Olivier Company‡ and Abdelouahab Zaatri§

†*Department of Mechanical Engineering, Faculty of Technology, Skikda University, Algeria*
‡*LIRMM UMR 5506 CNRS—UM2, 161 rue Ada, 34392 Montpellier Cedex 5, France*
§*Laboratory of Advanced Technologies, University of Constantine, Algeria*

(Accepted August 25, 2011. First published online: September 30, 2011)

SUMMARY

It is well known that Parallel Kinematic Mechanisms (PKMs) have an intrinsic dynamic potential (very high speed and acceleration) with high precision and high stiffness. Nevertheless, the choice of optimal dimensions that provide the best performances remains a difficult task, since performances strongly depend on dimensions. On the other hand, there are many criteria of performance that must be taken into account for dimensional synthesis, and which are sometimes antagonist. This paper presents an approach of multiobjective optimization for PKMs that takes into account several criteria of performance simultaneously that have a direct impact on the dimensional synthesis of PKMs. We first present some criteria of performance such as the workspace, transmission speeds, stiffness, dexterity, precision, as well as dynamic dexterity. Secondly, we present the problem of dimensional synthesis, which will be defined as a multiobjective optimization problem. The method of genetic algorithms is used to solve this type of multiobjective optimization problem by means of NSGA-II and SPEA-II algorithms. Finally, based on a linear Delta architecture, we present an illustrative application of this methodology to a 3-axis machine tool in the context of manufacturing of automotive parts.

KEYWORDS: Parallel robots; Parallel kinematic machine tool; Criteria of performance; Multiobjective optimization; Genetic algorithms NSGA-II and SPEA-II.

Notation

W:	Reachable workspace
P:	Vector of the variables of design
X:	Operational variables
q:	Motorized joints variables
ψ :	Passive joints variables
δq and δx:	Infinitesimal displacements
$\dot{q}$:	Joints velocities
$\dot{X}$:	Operational velocities
J :	Jacobian matrix
J^{-1} :	Inverse Jacobian matrix
J_x and J_q :	Two Jacobian sub-matrices
$J_{v,i}$:	Jacobian matrix of the translation of the body i
$J_{w,i}$:	Jacobian matrix of the orientation of the body i
κ_j :	Condition number of the matrix J^{-1}
$\sigma_{\max}(J^{-1})$:	The maximum singular value of J^{-1}
$\sigma_{\min}(J^{-1})$:	The minimum singular value of J^{-1}
η_j :	Index of global kinematic dexterity
η_M :	Index of global dynamic dexterity
Fe:	Amplification factors of Efforts
$Fe_{\min}$:	The minimum value of the amplification factors of Efforts
$Fe_{\max}$:	The maximum value of the amplification factors of Efforts
Fv :	Amplification factors of velocities
$Fv_{\min}$:	The minimum value of the amplification factors of velocities
$Fv_{\max}$:	The maximum value of the amplification factors of velocities
L_c :	Characteristic length
τ :	Joint forces
f :	Generalized forces
k_i :	Stiffness of the actuator
K:	Stiffness matrix
M:	Global inertia matrix of PKM
κ_M :	Condition number of mass matrix, M
R_i, R_j :	Radius of two segments i and j
L_i, L_j :	Length of two segments i *and* j
$x \prec y$:	x dominates y
k:	Elastic stiffness of the segments
m_i :	Body mass
v_{Gi} :	Translational velocity of the center of gravity of body i
w_{Gi} :	Angular velocity of the center of gravity of body i
I_i :	Inertia matrix of body i
N_c :	Number of bodies
m_1 :	Mass of each actuator
m_2 :	Mass of each segment (parallelogram)
m_3 :	Platform (Nacelle) mass

* Corresponding author. E-mail: Ridha.kelaiaia@lirmm.fr

https://doi.org/10.1017/S0263574711001032 Published online by Cambridge University Press

1. Introduction

Parallel Kinematic Mechanisms (PKMs) are the subject of many theoretical and applied research tasks.[1,2,3] These are a closed-loop kinematic chain whose end-effector is linked to the base by several kinematic chains. These present some advantages (intrinsic high dynamics, in particular) that lead them to be used in various industrial applications (assembly, handling, pick and place, machining, etc.). If the design and optimization are done efficiently, this helps to provide a high structural stiffness and a good balance of forces between the chains. Another key factor is the possibility to put the actuators close to fixed frame to minimize moving masses. This results in a higher payload and low inertia. Indeed, the ratio of payload with respect to the robot load is usually about $\frac{1}{10}$ for serial robots against $\frac{1}{2}$ for their parallel counterparts.[1]

In spite of the advantages of PKMs compared to conventional serial machines, their usability is still limited in the industry. This can be explained due to the following reasons (if the design and optimization are not well done in particular):

1. Limitation of their workspace (ratio between machine footprint and usable workspace).
2. Singularities inside their workspace, which involves large variability of the performances (workspace is not isotropic).
3. Complexity of transformations between operational and joint spaces (the complexity of direct geometrical models, which may not exist in analytical form).
4. Difficulties for decoupling movements into translations and rotations.

These previous issues represent fundamental problems for many researchers, which are interested in the design, optimization, and analysis of PKMs.

1.1. State of the art

In the last few years, an intensive effort has been devoted to optimizing PKM structures. In order to briefly situate the state of the art, some remarkable research has been done. In their work, Gosselin and Angeles[4] analyzed the optimal design of a planar 3-degrees of freedom (DOF) manipulator. They used different criteria such as the symmetry, the maximization of global workspace, and the isotropy of the Jacobian matrix of the manipulator. Gosselin and Lavoie[5] analyzed the isotropic configurations for a spherical 3-DOF parallel manipulator and found that the kinematic parameters of a manipulator could be adjusted to achieve an isotropic design. An approach using a genetic algorithm was proposed by Boudreau and Gosselin[6] to obtain the architectural parameters of the Stewart–Gough platform. This algorithm has been used to determine intersection between the actual workspace and the prescribed one. It has optimized 26 architectural parameters to minimize the area of non-intersecting regions.

In his doctoral thesis, Majoux[7] proposed the "Regular Dexterous Workspace (RDW): It's a part of Cartesian workspace whose shape is regular (cubic, cylinder, etc.) and the kinetostatic performances (condition number, transmission factor) are bounded inside the RDW." This concept has been used to optimize PKMs' geometry and compare several translational PKMs. He also proposed a method to improve translational PKMs' stiffness from influence analysis of geometrical parameters that did not modify the RDW volume.

A series of papers[4,5,8] have used the condition number of the Jacobian matrix as a criterion for optimization. When this number is equal to 1, the configuration is called isotropic. Yoshikawa[9,10] for the first time introduced this index for serial manipulators. Then Gosselin and Angeles[11,12] applied it to the PKMs to define the global performance index. They applied this criterion to both serial manipulators and ones with complex architecture, and observed that based on this index a numerical optimization should be applied.

Pittens and Podhorodeski[13] used the condition number only to quantify the dexterity of a manipulator. They analyzed various Stewart platform configurations that optimize local dexterity for determining optimal architecture and optimal operating points in the workspace. In their work, Jinsong and Xiaoqiang[14] analyzed the effects of design parameters on dexterity and workspace, and defined change ratios of the condition number, which have been used as an indicator to analyze the effects of design parameters on performances.

Some researchers have concentrated their work on the improvement of stiffness. Bhattacharya *et al.*[15] proposed a method where the concept of flexural stiffness over the workspace is used as the performance criterion.

Other papers[16,17] have focussed on the precision, which is also another major criterion for designing of fine movements such as machining operation, measurement, and so on. In their work, Wang and Masory,[18] by using the DH parameters, presented a kinematic model of error for the Stewart platform to minimize the effects of manufacturing tolerances, installation errors, and link offsets. In the same context, Patel and Ehmann[19] presented an error model of the Stewart platform, which is based on an error model formed through differentiation of kinematic equations. They proposed automated error analysis software, which graphically depicts position and orientation errors along tool paths and throughout the workspace. Obviously, it is necessary to take into account dynamics when determining PKMs' architectures. Several researchers have carried out this work. Ma and Angeles[20] determined the kinematic and inertial parameters of manipulator architecture using its generalized inertia matrix, which is isotropic for particular configurations. They proposed the notion of dynamic isotropy. Asada[21] presented the dynamics of a manipulator in operational space coordinates by constructing a Generalized Inertia Ellipsoid (GIE) in each point of the workspace. Change in the shape and orientation of this ellipsoid was related to nonlinear forces and coupling in manipulator dynamics. Toumi and Asada[22] and Yang and Tzeng[23] laid conditions that must be satisfied by kinematic parameters and inertial properties of a manipulator robot to obtain a decoupled and invariant tensor of inertia. Yoshikawa[24] developed a dynamic manipulability ellipsoid on the basis of end-effector acceleration and used its volume for the measurement of dynamic manipulability and performances of manipulators.

Another idea to optimize PKMs is to use a weighted criterion. Stock and Miller[25] used this method for the geometric synthesis of a linear Delta PKM. They formulated

https://doi.org/10.1017/S0263574711001032 Published online by Cambridge University Press

a function, which represents the sum of two indices based on manipulability and workspace. Zhang *et al.*[26] used a genetic algorithm to maximize stiffness and workspace of a tripod PKM. Another work used index of dexterity and avoidance of singularities to find optimal design. In their works, Klein and Blaho[27] used the index of dexterity and the avoidance of singularities for finding optimal design. Other researchers[28,29,30] have simultaneously considered the dexterity, the workspace and the stiffness in the designing of PKMs. Chablat *et al.*[31] proposed a numerical approach based on interval analysis for the design and comparison of 3-DOF PKMs. They used two criteria: a regular workspace shape and a kinetostatic performance index to find out the largest regular dexterous workspace enclosed in the Cartesian workspace. An algorithm describing this method was introduced. Julius *et al.*[32] optimized each objective function independent of other functions for the robotic-arm exoskeleton's torque capabilities by the modification of the key geometric design parameters. In addition, small works have proposed global approaches for designing of PKMs. Pritschow[33] proposed a systematic procedure in six steps for the designing of hexaglide or hexapod. Company and Pierrot,[34] following a global approach, developed a machine, UraneSX, for three-axis machining operations (drilling and taping for automotive industry).

The majority of the above works, based only on one or two criteria of performance, deal with the problem of dimensional synthesis of PKMs. In this paper, we will take into account and simultaneously study several criteria of performance that have a direct impact on the dimensional synthesis of PKMs. This leads to establish the dimensional synthesis as a multiobjective optimization issue. Therefore, some genetic algorithms will be used to solve this problem.

2. A Multiobjective Optimization Problem

In our approach, we consider the dimensional synthesis problem as a multiobjective optimization problem. Mathematically, the problem can be stated in the following form:

Find a vector $P^* = [p_1^*, p_2^*, \ldots\ldots, p_n^*]^T$
that **minimizes** $F(P) = [f_1(P), f_2(P), \ldots\ldots, f_k(P)]^T$
with $g_m(P) \leq 0$ (m constraints of inequality)
and $h_l(P) = 0$ (l constraints of equality).
$P^* \in^n$: vector of the decision variables,
$F(P^*) \in^k$: vector of the objectives function.

2.1. Definition of objective functions

In order to formulate a mathematical model as a multiobjective optimization problem, we consider the objective functions such as workspace, kinematic dexterity, speed and forces transmission, stiffness, precision, and dynamic dexterity. Then we will express each of these in the form of a mathematical function.

2.1.1. Workspace. The workspace "*W*" is one of the most important factors for designing PKMs. Theoretically, it is a set of space configurations that an end-effector can reach. This space is defined by its limits, which are imposed by joints (active and passive), lengths of segments, and internal collisions. A well-conditioned sub-workspace of the reachable workspace must be determined to guarantee a given level of performances. To this end, a method based on an optimization criterion, which is the condition number of the Jacobian matrix, is used to select only the points that guarantee a minimum value for this criterion. In other words, only the reachable points having a condition number lower than an imposed threshold will be retained to represent the sub-workspace. This procedure allows having a dextrous workspace (W_{dextrous}) in which the performances are better and more homogeneous, hence

$$W_{\text{dextrous}} \rightarrow \max. \tag{1}$$

2.1.2. Kinematic dexterity. It characterizes the ability of PKMs to perform very fine movements of translation and orientation (low amplitudes) with high accuracy. It is necessary to avoid small changes in the control (joint coordinates) that generate a big displacement of platform (end-effector). This dexterity can be evaluated by means of velocity equations of PKMs:

$$J_x \dot{X} = J_q \dot{q}. \tag{2}$$

So,

$$\dot{q} = J^{-1}\dot{X} = J_q^{-1} J_x \dot{X} \tag{3}$$

with $det(J_q) \neq 0$.

The inverse Jacobian matrix J^{-1} characterizes linear transformation between operational velocities and joint velocities; the quality of this transformation allows to analyze the kinematic dexterity of PKMs. The condition number of J^{-1} is used to measure the kinematic dexterity. It is defined as a ratio between the maximum and the minimum singular values of J^{-1}, which are, respectively, $\sigma_{\max}(J^{-1})$ and $\sigma_{\min}(J^{-1})$:

$$\kappa_J = \frac{\sigma_{\max}(J^{-1})}{\sigma_{\min}(J^{-1})} \in [1, \infty \tag{4}$$

When the condition number κ_J tends to infinity, the inverse Jacobian matrix J^{-1} becomes a singular matrix, and when $\kappa_J = 1$, it becomes a perfectly conditioned matrix, which is highly desirable. In this last case, the configurations are called isotropic. Therefore, our objective is

$$\begin{cases} \sigma_{\min}(J^{-1}) \rightarrow \max \\ \sigma_{\max}(J^{-1}) \rightarrow \min \end{cases}. \tag{5}$$

The objective function of kinematic dexterity is

$$\kappa_J \rightarrow \min. \tag{6}$$

It is noted that kinematic dexterity depends significantly on configuration and geometrical parameters of PKMs. It evolves inside the workspace; therefore, it is a local property.[35–37] To characterize it over the entire workspace, we use the global dexterity index η_J (used very often to compare various structures), which is defined by the average

https://doi.org/10.1017/S0263574711001032 Published online by Cambridge University Press

of local dexterity on the reachable workspace. It is given by the expression

$$\eta_J = \frac{\int_W \kappa_J \, dW}{\int_W dW} \rightarrow \min, \tag{7}$$

where W is the entire workspace volume.

(a) *Homogenization of the Jacobian matrix*

In case where the Jacobian matrix is composed of two Jacobian sub-matrices (one related to the position and another to the orientation), the elements are expressed in different units. As a direct consequence, the condition number does not have a physical sense. To solve this problem, we remove the dimensional non-homogeneity. The researchers have made several proposals. Angeles[36] suggested the use of "the characteristic length L_c," which is defined as the normalizing length that renders the Jacobian matrix dimensionless and its condition number to minimum at an optimum posture. It can be obtained by solving the constrained optimization problem (using numerical techniques), subject to geometrical constraints of the studied structure:

$$\min_P \kappa_J, \tag{8}$$

where P represents the vector of the variables of design. Another solution consists of using a constant dimension over all the workspace related to a dimension of the mobile platform or to integrate a weighting length based on the ratio between linear and angular speeds mentioned in the specifications.

(b) *Analysis of the singularities*

It is an essential operation before the determination of objective functions (criteria of performance) because the singular configurations are the ones where the performances of PKMs are degenerated and the structure may be damaged. Therefore, their determination becomes an indispensable task to avoid such situations. There are several methods used to determine these configurations (geometrical, algebraic, etc.). The method employed is the analysis of two Jacobian sub-matrices: J_q and J_x (see Eq. (2)); hence we distinguish the following cases:

$|J_x| = 0$: It is known as parallel singularity. This corresponds to the appearance of uncontrollable mobility of the end-effector because it is possible to move it, whereas the motorized joints are blocked. These singularities can exist inside the reachable workspace of the PKM, which presents additional difficulties for path planning. In these configurations the PKM gains one or more uncontrollable degrees of freedom and the stiffness of the PKM is lost locally.

$|J_q| = 0$: It is known as serial singularity. It is not possible to generate some velocities of the end-effector. These singularities represent the limits of the reachable workspace.[1] In these configurations the PKM loses one or more degrees of freedom.

$|J_x| = 0$ and $|J_q| = 0$: In this case the end-effector can move and actuators are blocked, and *vice versa*.

2.1.3. Velocity and force transmission. In order to evaluate the aptitude of PKMs to produce forces (forces and/or torques) or velocities (linear and/or angular) in different directions of the workspace, Wang *et al.*,[38] used the manipulability index (in velocity or in effort). This index can be represented by the manipulability ellipsoids[7,36](in velocity or effort).

The main axes of manipulability ellipsoid are the eigenvectors of $(JJ^T)^{-1}$ and the lengths of semi-axes (also called amplification factors of velocity or force), which are the singular values, $\sigma_i(J^{-1}) = \sqrt{\lambda_i((JJ^T)^{-1})}$. They are defined by the following relations:

$$Fv_{\min} = \frac{1}{Fe_{\max}} = \frac{1}{\sigma_{\max}(J^{-1})}, \tag{9}$$

$$Fv_{\max} = \frac{1}{Fe_{\min}} = \frac{1}{\sigma_{\min}(J^{-1})}. \tag{10}$$

We can remark that

$$\max(Fv_{\min}) \Leftrightarrow \min(Fe_{\max}) \Rightarrow \sigma_{\max}(J^{-1}) \rightarrow \min, \tag{11}$$

$$\min(Fv_{\max}) \Leftrightarrow \max(Fe_{\min}) \Rightarrow \sigma_{\min}(J^{-1}) \rightarrow \max. \tag{12}$$

According to Eqs. (9)–(12), the goal is to find the best compromise between Fv and Fe. We can note that this objective has a direct relation with the condition number of J^{-1} (see Eq. (2)), so the objective function is given by

$$\kappa_J \rightarrow \min. \tag{13}$$

To characterize it over the entire workspace, we use the global index η_J given by relation (7).

2.1.4. Accuracy. It is one of the most important criteria of PKMs. The errors on the actuators are transformed at the end-effector via the Jacobian matrix by the following relation:

$$\delta X = J \, \delta q. \tag{14}$$

This relation allows calculating the errors of the end-effector produced by the errors at the actuators. The amplification factors of δq are the singular values of the Jacobian matrix. In order to guarantee a good accuracy of PKMs, it is mathematically translated as

$$\sigma_{\max}(J) \rightarrow \min, \tag{15}$$

and

$$\sigma_{\max}(J) = \frac{1}{\sigma_{\min}(J^{-1})}. \tag{16}$$

Therefore, the objective function is given by

$$\sigma_{\min}(J^{-1}) \rightarrow \max \Leftrightarrow \kappa_J \rightarrow \min. \tag{17}$$

2.1.5. Stiffness. The value of the stiffness evolves according to the geometry, the topology of the structure, and the position and orientation of the end-effector within the workspace. The

https://doi.org/10.1017/S0263574711001032 Published online by Cambridge University Press

stiffness of a PKM at a given point of its workspace can be characterized by its stiffness matrix. This matrix combines the forces and torques applied to the end-effector (tool). It can be obtained using kinematic and static equations; a modification of the joint variable δq corresponds to the variation of the joint force,[1] $\delta\tau$ such that

$$\delta\tau = k\,\delta q, \tag{18}$$

where k represents the stiffness of the actuator,

$$\delta q = J^{-1}\,\delta X, \tag{19}$$

$$\delta f = J^{-T}\,\delta\tau. \tag{20}$$

If we replace Eqs. (18) and (19) in Eq. (20), we find

$$\delta f = k\,J^{-T}J^{-1}\delta X. \tag{21}$$

Therefore, the stiffness matrix K is given by

$$K = k\,J^{-T}J^{-1}, \tag{22}$$

$$K = k(J\,J^{T})^{-1}. \tag{23}$$

Generally, to evaluate the stiffness of PKMs, we take into account the stiffness of actuators; the other parts are considered as rigid bodies. The majority of PKMs have similar kinematic chains (this can reduce its costs), i.e., they have the same actuators, hence $k_1 = k_2 = \ldots\ldots = k_t = k$. The improvement of stiffness can be made by the analysis of the matrix $(J\,J^{T})^{-1}$, hence it is possible to estimate the minimum and maximum values of this stiffness by the calculation of eigenvalues of the matrix $(J\,J^{T})^{-1}$. The smallest value corresponds to the minimum and the largest one to the maximum of the stiffness.

The goal here is to have the best possible stiffness. This is obtained by

$$\sigma_{\min}(J^{-1}) \rightarrow \max \Leftrightarrow \kappa_J \rightarrow \min. \tag{24}$$

To characterize it over the entire workspace, we use the global index η_J given by relation (7).

Note: According to relations (12), (17), and (24), we note that the PKM can simultaneously carry out a task with good stiffness and accuracy but with slow velocity, and the opposite is also true, i.e., we cannot ensure a good control of the PKM at a very high velocity.

2.1.6. Dynamic dexterity. As in many types of mechanisms other than Cartesian, the non-linearity and the coupling of the equations of motion make the control of machines more difficult. However, with the current technological means, there is no lock. The variation of inertia seen by the actuators makes more complex the choice of actuators and control gains when we seek to reach high accelerations.

In order to enhance the dynamical performances, inertia must be minimized. In our case (dimensional synthesis), we will focus only on optimizing the inertia matrix, which is an important criterion to increase the dynamic capacities of PKMs.

Generally, the mass matrix (inertia matrix) of PKMs or robots can be obtained on the basis of their kinetic energy.[39,40] The kinetic energy of a rigid segment can be written as follows:

$$T_i = \frac{1}{2}\left(m_i v_{Gi}^{T} v_{Gi} + w_{Gi}^{T} I_i w_{Gi}\right), \tag{25}$$

with

$$v_{Gi} = J_{v,i}\dot{q},$$

$$w_{Gi} = J_{w,i}\dot{q},$$

where

$J_{v,\,i}$: Jacobian matrix of the translation of the ith body, and

$J_{w,\,i}$: Jacobian matrix of the orientation of the ith body.

Consequently, the kinetic energy of the PKM is the sum of the kinematic energies of all segments of the PKM:

$$T = \sum_{i=1}^{n} T_i, \tag{26}$$

$$T_i = \frac{1}{2}\dot{q}^{T}\left[\sum_{i=1}^{Nc}\left(m_i J_{v,i}^{T} J_{v,i} + J_{w,i}^{T} I_i J_{w,i}\right)\right]\dot{q}. \tag{27}$$

Hence, the mass matrix of the PKM is defined as

$$M = \left[\sum_{i=1}^{Nc}\left(m_i J_{v,i}^{T} J_{v,i} + J_{w,i}^{T} I_i J_{w,i}\right)\right]. \tag{28}$$

The evaluation of the dynamic performances is made according to the concept of GIE as proposed by Asada.[21] We can conclude that the movement of the end-effector can have a higher acceleration in the direction of the largest principal axis of this ellipsoid and a lower one in the direction of the smallest principal axis.

If the lengths of the two axes are identical, the performance of the accelerations is isotropic, which renders the dynamic dexterity better. The difference between the two lengths of the principal axis represents the anisotropy of the acceleration performance.

To make acceleration isotropic along all directions, it is strongly recommended to obtain a better dynamic dexterity. The condition number of the inertia matrix M used here to measure this dexterity is defined by

$$\kappa_M = \frac{\sigma_{\max}(M)}{\sigma_{\min}(M)} \in [1, \infty[\,. \tag{29}$$

The configurations where $\kappa_M = 1$ are called isotropic configurations. The objective function is defined as follows:

$$\kappa_M \rightarrow \min. \tag{30}$$

The dynamic dexterity, as well as kinematic dexterity, depends on the configuration and the geometrical parameters of PKMs. It varies within the workspace. To describe it on the whole reachable workspace by PKMs, we use the global dynamic dexterity index,[12,41] η_M, which is defined by

https://doi.org/10.1017/S0263574711001032 Published online by Cambridge University Press

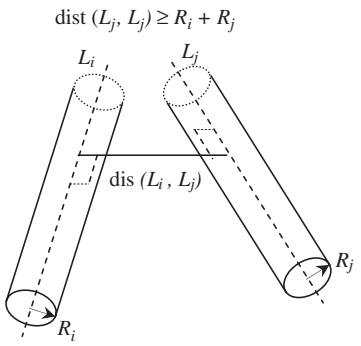


Fig. 1. Distance between two segments.

the average of the local dynamic dexterities over the entire workspace:

$$\eta_M = \frac{\int_W \kappa_M \, dW}{\int_W dW} \rightarrow \min. \tag{31}$$

2.2. Definition of constraints

2.2.1. Joints limits. These are represented by the motorized articulations

$$\rho_t^{\min} \leq \rho(x, p) \leq \rho_t^{\max}, \tag{32}$$

and the passive articulations

$$\psi_v^{\min} \leq \psi(x, p) \leq \psi_v^{\max}, \tag{33}$$

where
t: number of motorized articulations, and
v: number of passive articulations.

2.2.2. Distance between the segments of the mechanism (collision avoidance). Internal collisions between segments can occur as results in a smaller workspace. If we denote the radii and the lengths of two cylindrical segments i and j respectively by R_i, R_j and L_i, L_j (Fig. 1), then we can ensure that there is no mechanical interference if the distance between any pair of segments verifies by the following condition:[42]

$$\text{dist}(L_i, L_j) \geq R_i + R_j. \tag{34}$$

2.2.3. Technological constraints. Technological constraints include constraints such as actuators capacity, geometrical dimensions of the platform, the emplacement of PKMs in a machining line (manufacturing or assembly, for example), bulk of the machine, and so on.

2.3. Mathematical formulation of the problem

The formulation of the problem of optimal design based on the multiobjective optimization has a role to find the best dimensions of geometrical parameters of PKMs, which guarantees the best performances while satisfying the geometrical and technological constraints.

After analyzing the various performances criteria and their associated objective functions, we have established that they can be classified and represented as follows:

- Kinematic dexterity, transmission of velocities and forces, stiffness, and accuracy:

$$\eta_J = \frac{\int_W \kappa_J \, dW}{\int_W dW} \rightarrow \min.$$

- Dynamic dexterity:

$$\eta_M = \frac{\int_W \kappa_M \, dW}{\int_W dW} \rightarrow \min.$$

Finally, the problem of multiobjective optimization is formulated as follows:

$$\min F(P) = \min \begin{bmatrix} f_1 = n_J \\ f_2 = n_M \end{bmatrix}$$

such that the constraints

$$\rho_t^{\min} \leq \rho(x, p) \leq \rho_t^{\max},$$
$$\psi_v^{\min} \leq \psi(x, p) \leq \psi_v^{\max},$$

and

$$R_i + R_j \leq \text{dist}(L_i, L_j)$$

are satisfied.

3. Resolution Approaches

There are several techniques for solving this problem; the more usual one consists of treating successively the objectives. The result gives advantage to extreme solutions. Other techniques consist in transforming the multiobjective optimization problem into a mono-objective optimization problem, for which there exist various methods (goal attainment, method of compromise, etc.). The simplest is the method of weighted sum of objective functions. Its principle is to apply a weighting coefficient to each objective function and then to take the sum of the weighted objective functions to obtain a new unique objective function. Nevertheless, these methods cannot discover solutions hidden in concavities, as in some structural optimization problems it can behave catastrophically.

The appearance of new kind of methods, called metaheuristics, which include the simulated annealing method, ant colony algorithms, Tabu search and genetic algorithms, and so on. overcomes the problems encountered with conventional methods.

In our case, we selected genetic algorithms because of their good adequacy with our problem; they offer several advantages such as overcoming the obstacle of local minima (or maxima) and enabling the obtainment of the optimal Pareto front of a multiobjective optimization problem.

Among these algorithms, we propose to use two genetic algorithms called the Non-dominated Sorting-based Genetic Algorithm (NSGA-II) and the Strength Pareto Evolutionary Algorithm (SPEA-II). Both determine optimal Pareto fronts.

The Pareto optimality is based on the concept of dominance. For two criteria f_1 and f_2 (to simplify) the

https://doi.org/10.1017/S0263574711001032 Published online by Cambridge University Press

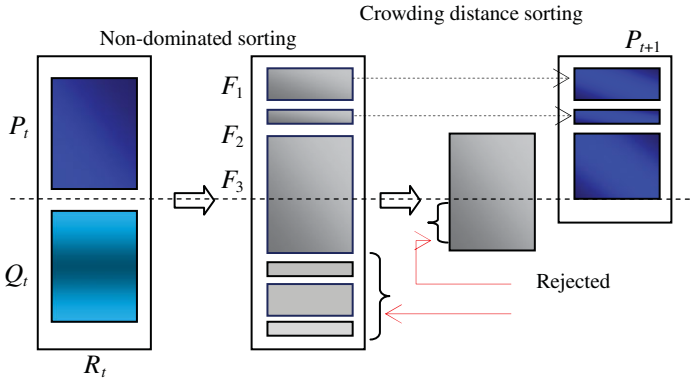


Fig. 2. (Colour online) A representation of NSGA-II.

solution x dominates another solution y:

$$(x \prec y) \quad \text{if } f_1(x) \leq f_1(y) \quad \text{and} \quad f_2(x) < f_2(y) \\ \text{or } f_1(x) < f_1(y) \quad \text{and} \quad f_2(x) \leq f_2(y) \quad .$$

A solution is not dominated or effective if no other solution dominates it: In other words, we cannot improve an objective without degrading another.

The optimization in the sense of Pareto consists in calculating all non-dominated solutions (or an approximation of this package), also called the Pareto front.

3.1. General principle of NSGA-II

The NSGA-II algorithm proposed by Deb *et al.*[43] is a new version of the NSGA algorithm. It is considered more effective than its predecessor because of the following:

- It uses an elitist approach that enables to safeguard the best solutions found in previous generations.
- It uses a sorting procedure based on the non-dominant (faster) criterion.
- It does not require any adjustment of parameter.
- It uses an operator of comparison based on calculation of the crowding distance. In the fist step of this algorithm, a population of parents (P_t) of size N and a child population (Q_t) of size N are assembled to form a population ($R_t = P_t \cup Q_t$) as shown in Fig. 2.

This assembly enables to ensure the elitism. The population of size $2N$ is then sorted according to a criterion of non-dominance to identify different fronts, F_1, F_2, and so on. The best individuals will find themselves in the first front. In the second step, a new parent population (P_{t+1}) is formed by adding the fronts (first front F_1, second front F_2, etc.) as long as those do not exceed N. If the number of individuals present in (P_{t+1}) is lower than (N), a procedure of crowding is applied on the first next front(F_i), not included in (P_{t+1}). The goal of this operator is to insert the ($N - |P_{t+1}|$) best individuals that miss in the population (P_{t+1}). The individuals of this front are used to calculate distance of crowding between two neighboring solutions. In the third step, once the individuals belonging to the population (P_{t+1}) are identified, a new child population (Q_{t+1}) is created by selection, crossing, and mutation. The selection by tournament is used but the criterion of the selection is now based on the operator of comparison.

The process continues from generation to generation, until a stopping criterion. The various stages described above are summarized in Table I.

3.2. General principle of SPEA-II

The SPEA-II algorithm proposed by Zitzler *et al.*[44] differs from its predecessor, the SPEA, by the size of fixed archive and the calculation of performance of individuals more refined. Moreover, only the individuals of the archive take part in the process of reproduction. The principal characteristics of this algorithm are as follows:

1. The quality of an individual is judged according to criteria of domination in the global population. More precisely, we affect to each individual, i, a value $S(i)$, which represents the number of individuals of the population that are dominated by i. The quality of the individual j is then obtained by adding the $S(i)$ for all individuals i that dominate j.
2. The estimation of the density is affected by the method inspired by that of the nearest neighboring solution: distances of all neighboring solutions are calculated and added to the quality of the individuals (described in the preceding paragraph) the inverse of the distance to the k^ith neighboring individual (generally k is fixed to 1).
3. The algorithm uses an archive of individuals of fixed size. In case of necessity, the sorting of the archive is done by removing the individual that has the nearest neighboring (in case of equality, we look at the second nearest neighboring). The principle of the SPEA-II is clarified by the following algorithm:
   - The inputs of the algorithm are as follows:
     N : Population size $\bar{N}$: Archive size
     T : Maximum number of generations
   - The output of the algorithm is
     A: The non-dominated set.
   - The steps of the algorithm are as follows:

Step 1. *Initialization*: Generate an initial population P_0 and create the empty archive $\bar{P}_0 = \Phi$ set $t = 0$.

Step 2. *Fitness assignment*: Calculate fitness values of individuals in P_t and $\bar{P}_t$.

Step 3. *Environmental selection*: Copy all non-dominated individuals in P_t and $\bar{P}_t$ to $\bar{P}_{t+1}$. If size of $\bar{P}_{t+1}$ exceeds $\bar{N}$ then reduce $\bar{P}_{t+1}$ by means of the truncation operator, otherwise if size of $\bar{P}_{t+1}$ is less than $\bar{N}$ then fill $\bar{P}_{t+1}$ with dominated individuals in P_t and $\bar{P}_t$.

Step 4. *Termination*: If $t \geq T$, or another stopping criterion is satisfied, then set A to the set of decision vectors represented by the non-dominated individuals in $\bar{P}_{t+1}$.

Step 5. *Mating selection*: Perform binary tournament selection with replacement on $\bar{P}_{t+1}$ in order to fill the mating pool.

4. Case Study: Application to the Linear Delta PKM

In this application, we apply the methodology developed for the dimensional synthesis of a linear Delta PKM (Fig. 3). Then we compare the results with the results obtained by Company and Pierrot[34] by analyzing its impact on the dextrous workspace, W_{dextrous} (the condition number of the inverse Jacobian matrix is used as a performance criterion).

https://doi.org/10.1017/S0263574711001032 Published online by Cambridge University Press

Table I. Process of the NSGA-II.

$R_t = P_t \cup Q_t$	Combine parent and children population
$F =$ fast, non-dominated-sort (R_t)	$F = (F_1, F_2, \ldots)$, all non-dominated fronts of R_t
$P_{t+1} = \Phi$ and $i = 1$	
Until $\lvert P_{t+1}\rvert + \lvert F_i\rvert \leq N$	Till the parent population is filled
Crowding-distance-assignment (F_i)	Calculate crowding distance in F_i
$P_{t+1} = P_{t+1} \cup F_i$	Include ith non-dominated front in the parent pop
$i = i + 1$	Check the next front for inclusion
Sort $(F_i, \prec_n)$	Sort in descending order using $\prec_n$
$P_{t+1} = P_{t+1} \cup F_i[1 : (N - \lvert P_{t+1}\rvert)]$	Choose the first $(N - \lvert P_{t+1}\rvert)$ elements of cal F_i
$Q_{t+1} =$ Make new-pop (P_{t+1})	Use selection, crossover, and mutation to create a new population, Q_{t+1}
$t = t + 1$	Increment the generation counter

4.1. Description and geometrical parametrization of PKM

This is a 3-DOF PKM in translation, type $3\mathbf{P}(\mathbf{S}\,\mathbf{S})_2$ (Fig. 4), using linear actuators connected to the base by sliding axis parallel to z_0. The PKM is mainly composed of a fixed base attached to a support (not represented) and a mobile platform.

The connection between the fixed base and the mobile platform is ensured by three identical kinematic chains arranged at an angle of 120°, each one of them consists of a linear actuator and two parallel bars of length L, with a ball joint at each end. The whole parallel bars and the two link arms are named parallelogram.

By construction we have,

$$\|A_{11}A_{12}\| = \|A_{21}A_{22}\| = \|A_{31}A_{32}\| = 2d,$$
$$\|B_{11}B_{12}\| = \|B_{21}B_{22}\| = \|B_{31}B_{32}\| = 2d,$$
$$\left\|A_{ij}B_{ij}\right\| = \|A_iB_i\| = L, \quad i = 1,\ 2,\ 3 \quad \text{and} \quad j = 1,\ 2.$$

It is important to note that the moving platform always remains parallel to the base.

The notations are as follows:

$R_0 = \{O_0, x_0, y_0, z_0\}$. The reference frame related to the base, such as "O_0" is the center of an equilateral triangle $O_1O_2O_3$ and at the same time the center of a circle of R_b radius.

$R_n = \{P, x_n, y_n, z_n\}$. The reference frame related to the moving platform, such as "P," is the center of an equilateral triangle $B_1B_2B_3$ and at the same time the center of a circle of R_n radius.

ρ_1, ρ_2, ρ_3. Articular parameter of the three linear actuators,

R_b: Radius of circle of center "O_0." It represents the distance between "O_0" and the points O_i: $\|O_0O_i\| = R_b \quad i = 1, 2, 3.$

R_n: Radius of circle of center "P." It represents the distance between "P" and the points B_i: $\|PB_i\| = R_n \quad i = 1, 2, 3.$

$X = \begin{bmatrix} x \\ y \\ z \end{bmatrix}$: Vector of the operational variables.

Our objective is to optimize the geometrical parameters (L, R_b, R_n) of this PKM (Fig. 3).

4.2. Kinematic model

The kinematic model of this PKM enables to express the relation between the situation of the end-effector $(xyz)^T$ with

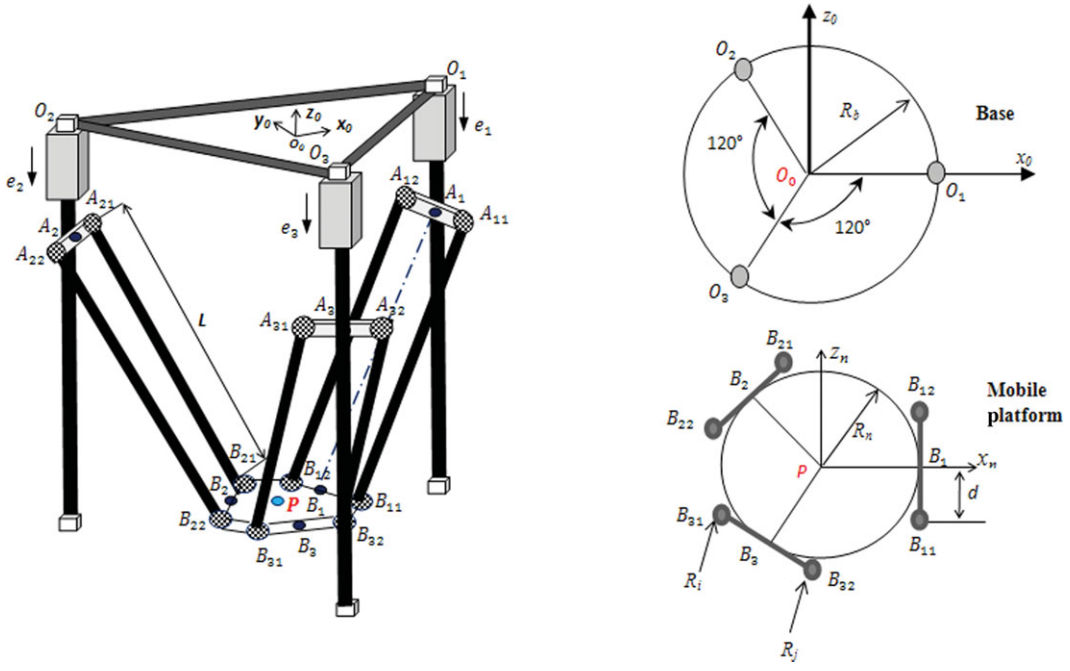


Fig. 3. (Colour online) Geometric description of linear Delta PKM.

https://doi.org/10.1017/S0263574711001032 Published online by Cambridge University Press

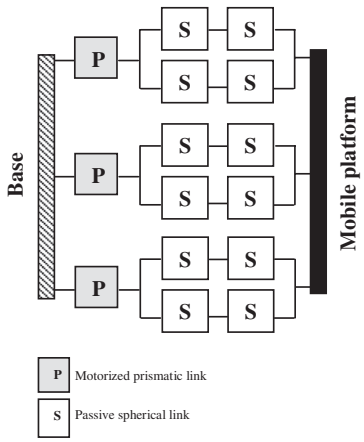


Fig. 4. Joints and loops graph of linear Delta PKM.

respect to a reference frame $R_0 = \{O_0, x_0, y_0, z_0\}$, knowing the joint variables of control $(\rho_1\ \rho_2\ \rho_3)^T$ and reciprocally.

The equations of constraints can be chosen as follows:

$$\|A_i B_i\| = L, \quad i = 1, 2, 3. \tag{35}$$

The coordinates of points B_i in the reference frame related to the platform (nacelle) are given by

$$[B_i]_{na} = \begin{bmatrix} R_n \cos\alpha_i \\ R_n \sin\alpha_i \\ 0 \end{bmatrix}, \tag{36}$$

where α_i: angle between the ith actuator and the plane of the fixed base, i.e., between $\boldsymbol{x}_0$ and $\boldsymbol{x}_i$ around axis z, its value is equal to $\frac{2\pi}{3}(i-1)$; $i = 1, 2, 3$.

In the reference frame related to the base

$$[B_i]_{\text{base}} = \begin{bmatrix} R_n \cos\alpha_i \\ R_n \sin\alpha_i \\ 0 \end{bmatrix} + \begin{bmatrix} x \\ y \\ z \end{bmatrix} = \begin{bmatrix} x + R_n \cos\alpha_i \\ y + R_n \sin\alpha_i \\ z \end{bmatrix}. \tag{37}$$

The coordinates of points A_i in the reference frame related to the base are given by

$$[A_i]_{\text{base}} = \begin{bmatrix} R_b \cos\alpha_i \\ R_b \sin\alpha_i \\ \rho_i \end{bmatrix}. \tag{38}$$

Hence,

$$(x - (R_b - R_n)\cos\alpha_i)^2 + (y - (R_b - R_n)\sin\alpha_i)^2 + (z - \rho_i)^2 = L^2. \tag{39}$$

Equation (39) is used to establish the expression of the inverse kinematic model:

$$\begin{cases} \rho_1 = z \mp \sqrt{L^2 - (x + R_n - R_b)^2 - y^2}, \\ \rho_2 = z \\ \quad \mp \sqrt{L^2 - \left(x + \frac{1}{2}(R_b - R_n)\right)^2 - \left(y + \frac{\sqrt{3}}{2}(R_n - R_b)\right)^2}, \\ \rho_3 = z \\ \quad \mp \sqrt{L^2 - \left(x + \frac{1}{2}(R_b - R_n)\right)^2 - \left(y + \frac{\sqrt{3}}{2}(R_b - R_n)\right)^2}. \end{cases} \tag{40}$$

The sign admitted in the system of Eq. (40) is "+" because it corresponds well to the configuration represented in Fig. 3.

For the establishment of the direct kinematic model, we solve the system (40) with respect to x, y, and z, which yields the following system:

$$\begin{cases} Fz^2 + 2Gz + H = 0 \\ y = Az + B \\ x = Cz + D \end{cases}. \tag{41}$$

Hence,

$$\begin{cases} z_1 = \dfrac{-G - \sqrt{G^2 - F.H}}{F}, \\ z_2 = \dfrac{-G + \sqrt{G^2 - F.H}}{F}. \end{cases} \tag{42}$$

The adopted solution is $z = \min(z_1, z_2)$, with

$$A = \frac{(\rho_2 - \rho_3)}{\sqrt{3}(R_n - R_b)}, \quad C = \frac{2(\rho_2 - \rho_1) - A\sqrt{3}(R_n - R_b)}{\sqrt{3}(R_b - R_n)},$$
$$B = \frac{\left(\rho_3^2 - \rho_2^2\right)}{2\sqrt{3}(R_n - R_b)}, \quad D = \frac{\rho_1^2 - \rho_2^2 - B\sqrt{3}(R_n - R_b)}{3(R_b - R_n)},$$
$$E = R_n - R_b + B, \quad F = A^2 + C^2 + 1,$$
$$G = A.E + C.D - \rho_1, \quad H = E^2 + D^2 + \rho_1^2 - L^2.$$

4.3. Jacobian matrix and singularity analysis

We differentiate Eq. (39) with respect to time and obtain the following expression:

$$(x - (R_b - R_n)\cos\alpha_i)\dot{x} + (y - (R_b - R_n)\sin\alpha_i)\dot{y} + (z - \rho_1)\dot{z} = (z - \rho_i)\dot{\rho}_i. \tag{43}$$

In matrix form, the system is written as

$$J_x \begin{bmatrix} \dot{x} \\ \dot{y} \\ \dot{z} \end{bmatrix} = J_\rho \begin{bmatrix} \dot{\rho}_1 \\ \dot{\rho}_2 \\ \dot{\rho}_3 \end{bmatrix}, \tag{44}$$

https://doi.org/10.1017/S0263574711001032 Published online by Cambridge University Press

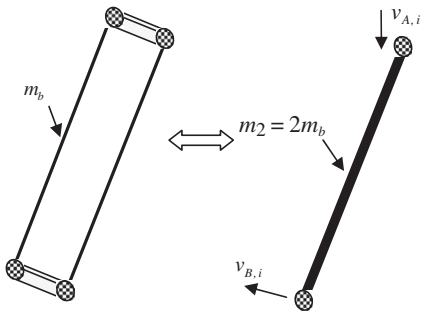


Fig. 5. Simplification of a parallelogram.

where

$$J_x = \begin{bmatrix} x - (R_b - R_n) & y & z - \rho_1 \\ x + \frac{1}{2}(R_b - R_n) & y - \frac{\sqrt{3}}{2}(R_b - R_n) & z - \rho_2 \\ x + \frac{1}{2}(R_b - R_n) & y + \frac{\sqrt{3}}{2}(R_b - R_n) & z - \rho_3 \end{bmatrix},$$

$$J_\rho = \begin{bmatrix} z - \rho_1 & 0 & 0 \\ 0 & z - \rho_2 & 0 \\ 0 & 0 & z - \rho_3 \end{bmatrix},$$

and

$$J^{-1} = J_\rho^{-1} J_x. \tag{45}$$

The analysis of the inverse Jacobian matrix enables us to avoid singular configurations, thus we can distinguish the following cases.

4.3.1. Serial singularities ($|J_\rho| = 0$) $|J_\rho| = 0 \Rightarrow (z - \rho_1)(z - \rho_2)(z - \rho_3) = 0 \Rightarrow z = \rho_1 \vee z = \rho_2 \vee z = \rho_3$. This singularity appears when one or two, or even three parallelograms become perpendicular to the directions of linear actuators: $A_i B_i \perp e_i$ (Fig. 3).

4.3.2. Parallel singularities ($|J_x| = 0$) $|J_x| = 0 \Rightarrow (R_b - R_n)\,[P_1 x + P_2 y + P_3 z + P_4] = 0$. where, $P1 = \frac{\sqrt{3}}{2}(-2\rho_1 + \rho_2 + \rho_3)$, $P_2 = \frac{3}{2}(\rho_3 - \rho_2)$, $P3 = \frac{3\sqrt{3}}{2}(R_b - R_n)$, and $P_4 = \frac{\sqrt{3}}{2}(\rho_1 + \rho_2 + \rho_3)\,(R_b = R_n)$. We distinguish the following two cases:

- $R_b - R_n = 0$, i.e., the diameter of the base is equal of the diameter of the platform to take into account the design.
- The parallel singularities represent the Cartesian plane in the space whose equation is represented by $P_1 x + P_2 y + P_3 z + P_4 = 0$.

This singularity appears when three parallelograms are coplanar; to avoid it, it is enough to choose "L" such as $L > (R_b - R_n)$.

4.4. Mass matrix

In order to determine the mass matrix, we consider each parallelogram as a single segment (Fig. 5), and we suppose that the velocities of the two ends are, respectively, $v_{A,\,i}$ and $v_{B,\,i}$, where $v_{A,\,i}$ is the velocity of the ith actuator and $v_{B,\,i}$ is the velocity of the mobile platform. These are given by the following expressions:

$$v_{A,i} = \begin{bmatrix} 0 \\ 0 \\ 1 \end{bmatrix} \dot{\rho}_i,$$

$$v_{A,1} = \begin{bmatrix} 0 & 0 & 0 \\ 0 & 0 & 0 \\ 1 & 0 & 0 \end{bmatrix} \dot{\rho} = J_{A,1}\dot{\rho},$$

$$v_{A,2} = \begin{bmatrix} 0 & 0 & 0 \\ 0 & 0 & 0 \\ 0 & 1 & 0 \end{bmatrix} \dot{\rho} = J_{A,2}\dot{\rho}$$

$$v_{A,3} = \begin{bmatrix} 0 & 0 & 0 \\ 0 & 0 & 0 \\ 0 & 0 & 1 \end{bmatrix} \dot{\rho} = J_{A,3}\dot{\rho},$$

$$v_{B,1} = v_{B,2} = v_{B,3} = \begin{bmatrix} \dot{x} \\ \dot{y} \\ \dot{z} \end{bmatrix} = J\dot{\rho}.$$

Hence,

- The kinetic energy of each segment (parallelogram) is

$$T_{s,i} = \frac{1}{2} m_2 \left[\frac{1}{3} \left(v_{A,i}^2 + v_{B,i}^2 + v_{A,i} v_{B,i} \right) \right],$$

$$T_{s,i} = \frac{1}{2} m_2 \dot{\rho}^T \left[\frac{1}{3} \left(J_{A,i}^T J_{A,i} + J^T J + J_{A,i}^T J \right) \right] \dot{\rho}.$$

- The kinetic energy of each actuator is

$$T_{a,i} = \frac{1}{2} m_1 v_{A,i}^2 = \frac{1}{2} m_1 \dot{\rho}^T J_{A,i}^T J_{A,i} \dot{\rho}.$$

- The kinetic energy of the mobile platform is

$$T_{na} = \frac{1}{2} m_{na} v_{na}^2 = \frac{1}{2} m_{na} \dot{\rho}^T J^T J \dot{\rho}.$$

Consequently, the kinetic energy of the PKM is

$$T = \frac{1}{2} \dot{\rho}^T \left[m_1 \sum_{i=1}^{3} J_{A,i}^T J_{A,i} + m_2 \sum_{i=1}^{3} \frac{1}{3} \left(J^T J + J_{A,i}^T J_{A,i} + J_{A,i}^T J \right) + m_{na} J^T J \right] \dot{\rho}.$$

Hence, the mass matrix of the PKM is

$$M = m_1 \sum_{i=1}^{3} J_{A,i}^T J_{A,i} + m_2 \sum_{i=1}^{3} \frac{1}{3} \left(J^T J + J_{A,i}^T J_{A,i} + J_{A,i}^T J \right) + m_{na} J^T J.$$

https://doi.org/10.1017/S0263574711001032 Published online by Cambridge University Press

Table II. Limits of the dextrous workspace.

Condition number κ_J	NSGA-II and SPEA-II			Company and Pierrot[34]		
	x (m)	y (m)	z (m)	x (m)	y (m)	z (m)
$\kappa_J \leq 2.86 \left(\frac{1}{\kappa_J} \geq 0.35\right)$	$x_{min} = -0.17$	$y_{min} = -0.21$	$z_{min} = -1.12$	$x_{min} = -0.32$	$y_{min} = -0.38$	$z_{min} = -1.42$
	$x_{max} = 0.24$	$y_{max} = 0.21$	$z_{max} = -0.50$	$x_{max} = 0.42$	$y_{max} = 0.38$	$z_{max} = -0.85$
$\kappa_J \leq 2.22 \left(\frac{1}{\kappa_J} \geq 0.45\right)$	$x_{min} = -0.14$	$y_{min} = -0.17$	$z_{min} = -1.2$	$x_{min} = -0.075$	$y_{min} = -0.085$	$z_{min} = -1.42$
	$x_{max} = 0.20$	$y_{max} = 0.17$	$z_{max} = -0.50$	$x_{max} = 0.085$	$y_{max} = 0.085$	$z_{max} = -0.085$
$\kappa_J \leq 1.82 \left(\frac{1}{\kappa_J} \geq 0.55\right)$	$x_{min} = -0.12$	$y_{min} = -0.13$	$z_{min} = -1.12$	–	–	–
	$x_{max} = 0.15$	$y_{max} = 0.13$	$z_{max} = -0.50$			

4.5. Formulation of the optimization problem

In this example, the PKM has the square Jacobian matrix of dimension (3, 3) and it does not require homogenization because the movement of the platform is only in translation, so the geometrical parameters to optimize are the dimensions of the PKM «R_b, R_n and L».

According to the models developed previously, we find that the influences of «R_b and R_n» on kinematics and dynamics are coupled (see expressions of the inverse kinematic model, Jacobian, and mass matrix). Consequently, the geometrical magnitude that we take into account is the difference $(R_b - R_n)$.

In addition, some constraints of the bulk of the machine limit the values of these parameters as the external diameter of electro-spindle, which imposes a minimal value $(R_n)_{\min} = 0.15\,\text{m}$. Moreover, the PKM should have a small bulk (including actuators) considering its location in a production chain transfer,[34] from where $(R_b)_{\max} = 0.70\,\text{m}$. The parameter «$L$» remains free to optimize.

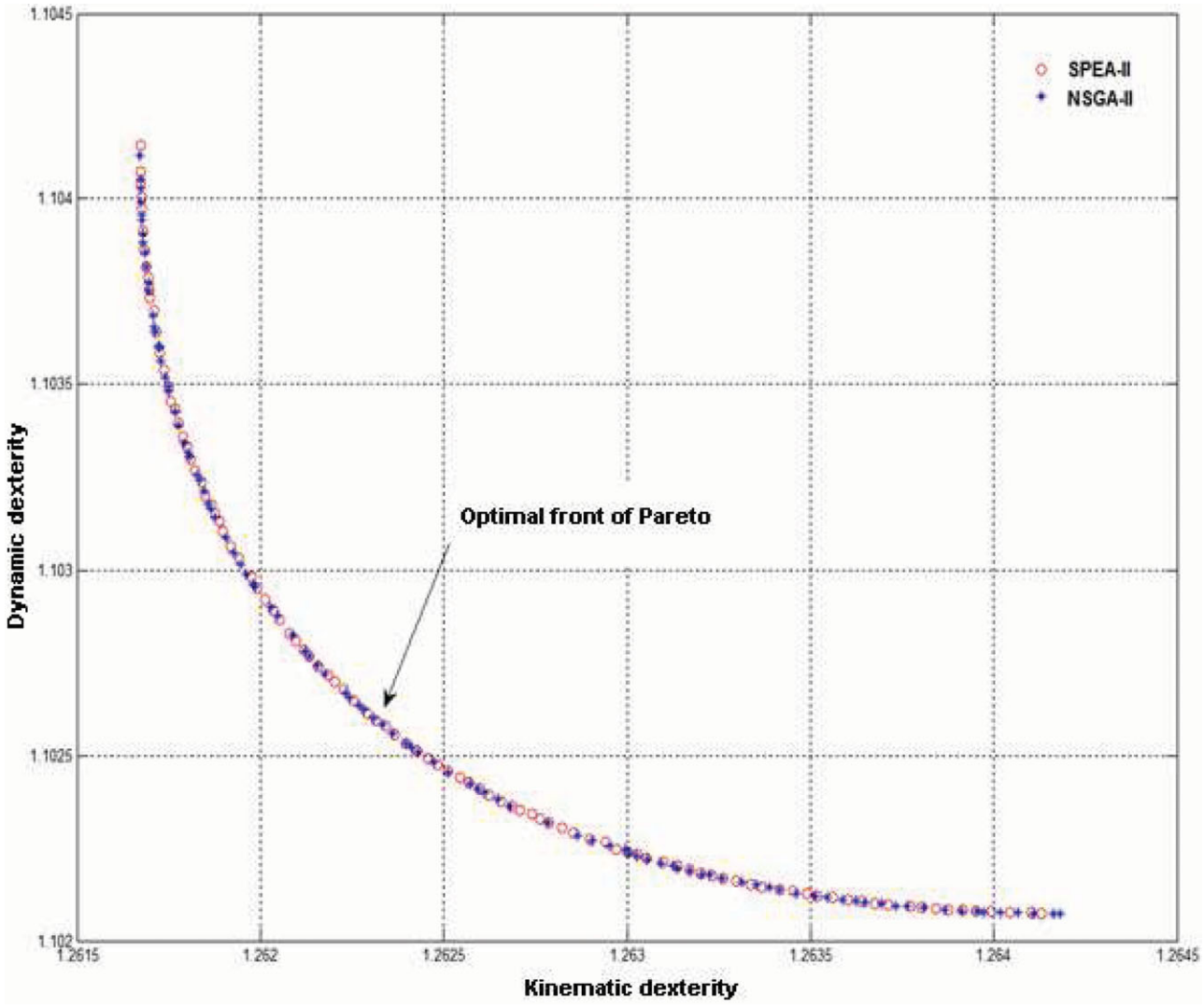


Fig. 6. (Colour online) Optimal front of Pareto.

https://doi.org/10.1017/S0263574711001032 Published online by Cambridge University Press

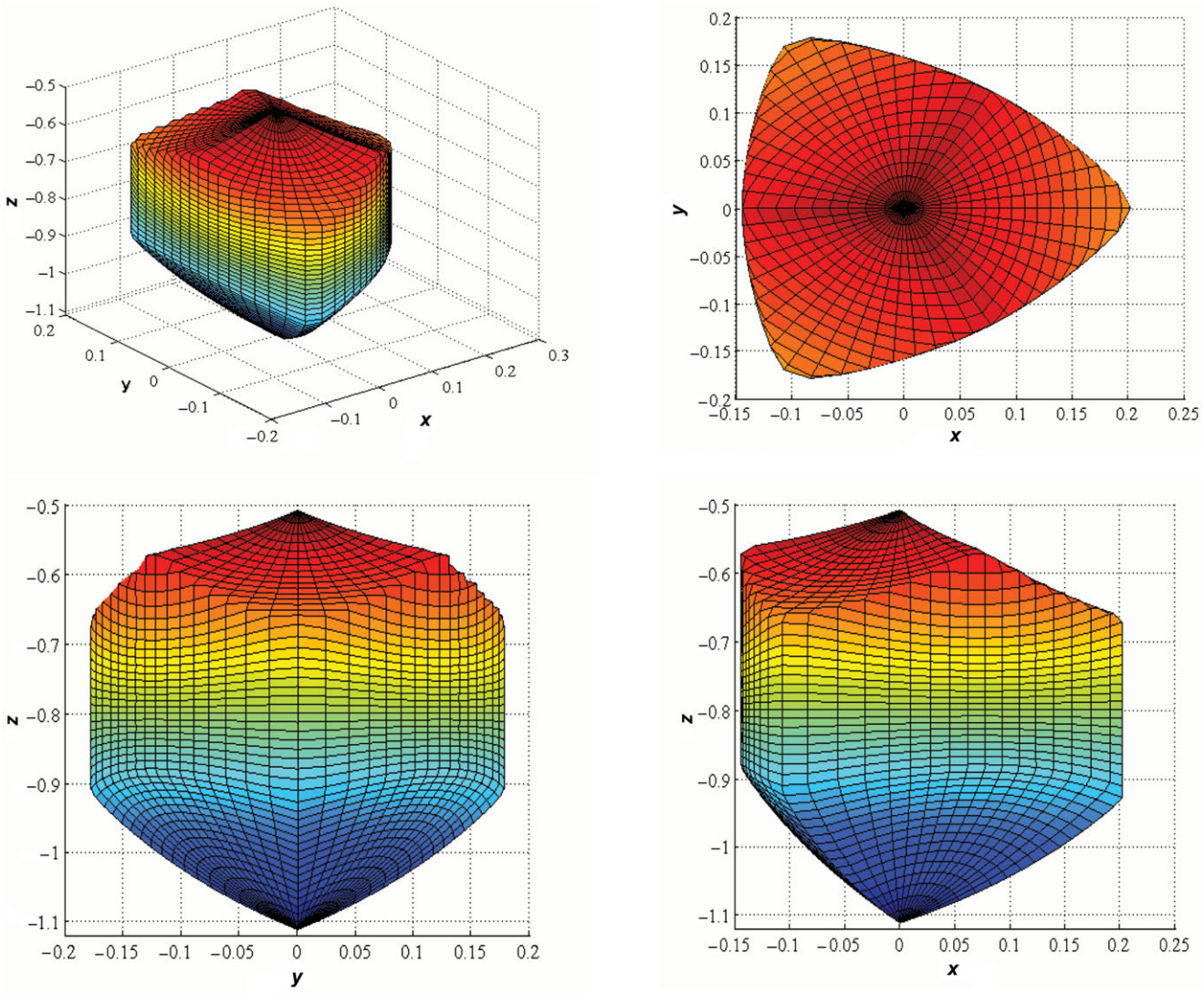


Fig. 7. (Colour online) Workspace with the constraints $1/\kappa_J \geq 0.45$ when $L = 0.750$ m.

The multiobjective optimization problem can be formulated as

$$\min F(P) = \min \begin{bmatrix} f_1 = n_J \\ f_2 = n_M \end{bmatrix}$$

with $P = \begin{bmatrix} R_b - R_n \\ L \end{bmatrix}$: vector of geometrical parameters, such that the constraints

$$\begin{aligned} 0 \leq |\rho_i| \leq 0.600\,\text{m} \qquad & i = 1, 2, 3, \\ R_b - R_n < L, & \\ 0.150\,\text{m} \leq R_b - R_n \leq 0.550\,\text{m}, & \\ 0.750\,\text{m} \leq L \leq 1.500\,\text{m}, & \\ (R_i + R_j) \leq d = 0.100\,\text{m}, & \\ m_1 = m_{na} = 50\,\text{kg}, & \\ m_2 = 10\,\text{kg} & \end{aligned}$$

are satisfied.

4.6. Results and discussion

Matlab is used for the implementation of the NSGA-II and SPEA-II with the following parameters: number of population = 100, number of generation = 100, crossing probability = 0.9, and probability of mutation = 0.1.

Figure 6 represents the optimal Pareto front obtained between the criteria of performance (the kinematic dexterity, the transmission of velocities and forces, stiffness, and accuracy) represented by η_J and the dynamic dexterity represented by η_M. We notice that the optimal Pareto fronts obtained by applying the two algorithms NSGA-II and SPEA-II are almost the same. The geometric parameters, which correspond to the two fronts, are practically the same:

$$\begin{bmatrix} R_b - R_n \\ L \end{bmatrix} = \begin{bmatrix} 0.550\,\text{m} \\ 0.750\,\text{m} \end{bmatrix}.$$

We also note that both fronts are obtained when the difference $(R_b - R_n)$ increases from where we should have $(R_b - R_n)$ the greatest possible and when the length «L » of segments decreases, from where the chosen «L» must be as small as possible.

https://doi.org/10.1017/S0263574711001032 Published online by Cambridge University Press

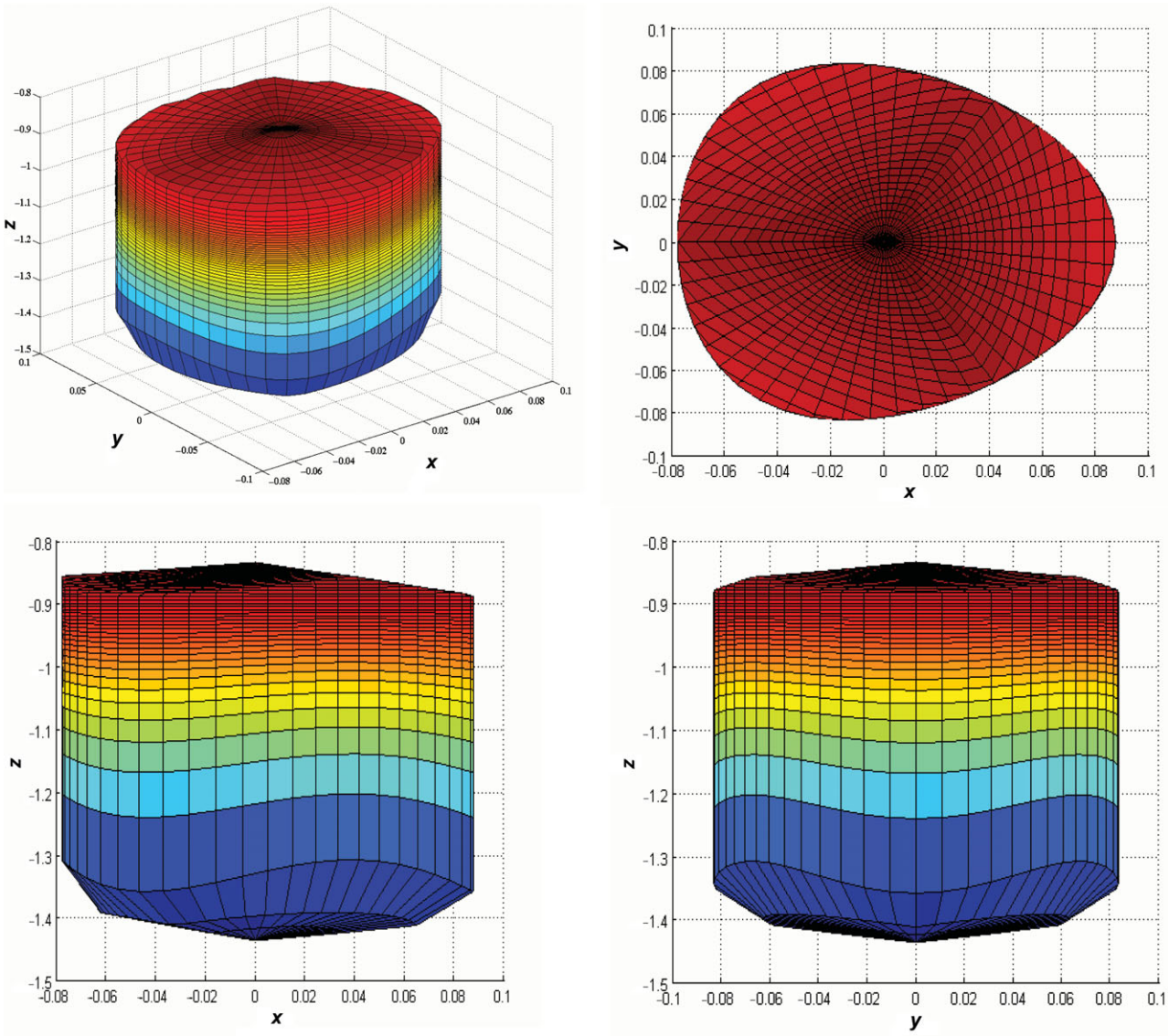


Fig. 8. (Colour online) Workspace with the constraints $1/\kappa_J \geq 0.45$ when $L = 1.000$ m.

4.7. Analysis of dexterous workspace

After taking account of several criteria of performance in developed methodology, we present in this section its impact on the dextrous workspace (optimized according to a kinetostatic criterion: the condition number of the inverse Jacobian matrix), which presents this workspace with the geometrical parameters $P = \begin{bmatrix} R_b - R_n \\ L \end{bmatrix} = \begin{bmatrix} 0.550\,\text{m} \\ 0.750\,\text{m} \end{bmatrix}$ obtained with methodology developed above. Then we compare it with the dextrous workspace obtained with the geometrical parameters obtained by Company and Pierrot[34] where $P = \begin{bmatrix} R_b - R_n \\ L \end{bmatrix} = \begin{bmatrix} 0.550\,\text{m} \\ 1.000\,\text{m} \end{bmatrix}$.

The workspace of PKM is obtained by the intersection of three cylinders whose axes are parallel the z-axis.

We note here that the minimum value of condition number J^{-1} obtained on the whole workspace with dimensions of Company and Pierrot[34] is $(\kappa_J)_{\min} = 1.990$ and by the method of the genetic algorithms the value is $(\kappa_J)_{\min} = 1.265$.

Table II represents the limits of the dextrous workspace according to the value of κ_J obtained with the geometrical parameters $P = \begin{bmatrix} R_b - R_n \\ L \end{bmatrix} = \begin{bmatrix} 0.550\,\text{m} \\ 0.750\,\text{m} \end{bmatrix}$ (obtained with the genetic algorithms NSGA-II and SPEA-II) and $P = \begin{bmatrix} R_b - R_n \\ L \end{bmatrix} = \begin{bmatrix} 0.550\,\text{m} \\ 1.000\,\text{m} \end{bmatrix}$ (obtained by Company and Pierrot[34]).

According to Table II, we note that when the values of κ_J are minimized so that $(\kappa_J \to 1)$, the dextrous workspace obtained with parameters obtained by genetic algorithms becomes increasingly larger than that obtained with Company and Pierrot's[34] parameters.

Figure 7 presents the dextrous workspace when $\kappa_J \leq 2.22(\frac{1}{\kappa_J} \geq 0.45)$ and with the geometrical parameters $P = \begin{bmatrix} R_b - R_n \\ L \end{bmatrix} = \begin{bmatrix} 0.550\,\text{m} \\ 0.750\,\text{m} \end{bmatrix}$ (obtained by genetic algorithms) in space (xyz) and three plans (xy), (xz), and (yz) for better visualization.

https://doi.org/10.1017/S0263574711001032 Published online by Cambridge University Press

Figure 8 presents the dextrous workspace when $\kappa_J \leq 2.22(\frac{1}{\kappa_J} \geq 0.45)$ and with the geometrical parameters $P = \begin{bmatrix} R_b - R_n \\ L \end{bmatrix} = \begin{bmatrix} 0.550\,\text{m} \\ 1.000\,\text{m} \end{bmatrix}$ (obtained by Company and Pierrot[34]) in space *(xyz)* and three plans (*xy*), (*xz*), and (*yz*).

We note here that the shape of the dextrous workspace obtained with both methods is shaped irregularly, but from the dimensions given in Table II, we can obtain a dextrous workspace with regular shape as parallelepiped, cubic, cylinder, and so on by optimizing the dimensions of the form that we desire to obtain.

5. Conclusion

In this paper, we have presented a methodology of dimensional design of PKMs based on an approach of multiobjective optimization by genetic algorithms. In order to be implemented (done), we have introduced and discussed several indices (criteria) of performance, which intervene in the dimensioning of PKMs such as the workspace, kinematic dexterity, the factors of transmission velocity and effort, the precision, stiffness, and dynamic dexterity. Then we have defined the objective functions from the criteria of performance, the constraints, and the variables (geometrical parameters) that allow formulating mathematically the multiobjective optimization problem, and for its resolution (approach of resolution), we have chosen two genetic algorithms, the NSGA-II and the SPEA-II. To test the efficiency of this methodology, we have applied it to a linear Delta PKM (three axes), which was also the object of dimensional synthesis studied by Company and Pierrot.[34]

The proposed approach allows determining a good approximation of the compromise (front of Pareto) between the various criteria of performance (sometimes antagonistic), which is very difficult to obtain with the classical methods that cannot take into account all these criteria simultaneously.

Furthermore, the comparison between the results obtained by this methodology and those obtained by the method presented in ref. [34] reveals concordant results (very appreciable).

Indeed, the optimal dimensions obtained respect the various criteria of performance to have a larger dextrous workspace (where the performances are better).

Thus, taking into account the generic approach to model this problem and the results obtained, it remains as a prospect to generalize this methodology of design to other PKMs with more complex structures.

References

1. J.-P. Merlet, *Parallel Robots*, 2nd ed. (Springer, Heidelberg, Germany, 2006).
2. J.-P. Merlet, "Designing a parallel manipulator for a specific workspace," *Int. J. Robot. Res*. **16**(4), 545–556 (1997).
3. J. Schönherr, "Evaluation and Optimum Design of Parallel Manipulators Having Defined Workspace," **In**: *Proceedings of the DECTC*, Baltimore, Maryland (Sep. 10–13, 2000) pp. 1–9.
4. C. Gosselin and J. Angeles, "The optimum kinematic design of a planar three-degree-of-freedom parallel manipulator," *ASME J. Mech. Transm. Autom. Des.* **110**, 35–41 (Mar. 1988).
5. C. Gosselin and E. Lavoie, "On the kinematic design of spherical three-degree-of-freedom parallel manipulator," *Int. J. Robot. Res*. **12**(4), 394–402 (Aug. 1993).
6. R. Boudreau and C. Gosselin, "La synthèse d'une plate-forme de Gough-Stewart pour un espace atteignable prescrit," *Mech. Mach. Theory* **36**, 327–342 (2001).
7. F. Majoux, "Analyse cinétostatique des machines parallèles à translation," *Thèse de Doctorat* (Ecole centrale de Nante, France, Nov. 2004).
8. K. E. Zanganeh and J. Angeles, "Kinematic isotropy and the optimum design of parallel manipulators," *Int. J. Robot. Res*. **16**(2), 185–197 (1997).
9. T. Yoshikawa, *Foundations of Robotics: Analysis and Control* (MIT Press, Cambridge, MA, 1990).
10. T. Yoshikawa, "Manipulability of robotic mechanism," *Int. J. Robot. Res.* **4**(2), 3–9 (1985).
11. C. Gosselin and J. Angeles, "Singularly analysis of closed loop kinematic chains," *ASME J. Mech. Des.* **112**(3), 331–336 (1990).
12. C. Gosselin and J. Angeles, "A Global performance index for the kinematic optimisation of robotic manipulators," *J. Mech. Des.* **113**, 220–226 (Sep. 1991).
13. K. H. Pittens and R. Podhorodeski, "A family of platforms with optimal dexterity," *J. Robot. Syst.* **10**(4), 463–479 (1993).
14. W. Jinsong and T. Xiaoqiang, "Analysis and dimensional design of a novel hybrid machine tool," *Int. J. Mach. Tools Manuf.* **43**, 647–655 (2003).
15. S. Bhattacharya, H. Htval and A. Gosh, "On the optimum design of Stewart platform type parallel manipulator," *Robotica* **13**, 133–140 (1995).
16. C.-S. Han, D. Tesar and A. Traver "The Optimum Design of a 6 DOF Fully Parallel Micromanipulator for Enhanced Robot Accuracy," **In**: *Proceedings of ASME Design Automation Conference*, Montréal (Sep. 17–20, 1989), pp. 357–363.
17. J. Ryu and J. Cha "Volumetric error analysis and architecture optimization for accuracy of HexaSlide type parallel manipulators," *Mech. Mach. Theory*, **38**(3), 227–240 (2003).
18. J. Wang and O. Masory, "On the Accuracy of a Stewart Platform – Part I. The Effect of Manufacturing Tolerances," **In**: *Proceedings of the IEEE International Conference on Robotics Automation*, Atlanta, Georgia (May 1993) pp. 114–120.
19. A. J. Patel and K. F. Ehmann, "Volumetric error of a Stewart platform-based machine tool," *Ann. CIRP* **46**, 287–290 (1997).
20. O. Ma and J. Angeles, "Optimal Design of Manipulator under Dynamic Isotropy Conditions," **In**: *Proceeding of the IEEE International Conference on Robotics and Automation*, Atlanta Georgia (May 1993) pp. 470–475.
21. H. Asada, "A geometrical representation of manipulator dynamics and its application to arm design," *ASME J. Dyn. Sys. Meas. Control* **105**, 131–135, 142 (1983).
22. Y. Toumi and H. Asada, "The Design of Arm Linkages with Decoupled and Configuration Invariant Inertia Tensors – Part I and II," **In**: *Proceedings of the ASME Winter Annual Meeting, Robotics and Manufacturing Automation Symposium,* Wam, Miami (Nov. 1985) pp. 145–161.
23. D. C. H Yang and S. W. Tzeng, "Simplification and linearization of manipulator dynamics by the design of inertia distribution," *Int. J. Robot. Res.* **5**(3), 120–128 (1986).
24. T. Yoshikawa, "Dynamic manipulability of robot manipulators," *Int. J. Robot. Res.* **2**(1), 113–124 (1985).
25. M. Stock and K. Miller, "Optimal kinematic design of spatial parallel manipulator: Application to linear delta robot," *ASME J. Mech. Des.* **125**, 292–301 (June 2003).
26. D. Zhang, Z. Xu, C. M. Mechefske and F. Xi, "Design Optimization of Parallel Kinematic Toolheads with Genetic Algorithms," 3rd Parallel Kinematic Seminar, PKS International Conference, Chemnitz, Germany (Apr. 23–25, 2002).
27. C. A. Klein and B. E. Blaho, "Dexterity measures for the design and control of kinematically redundant manipulators," *Int. J. Robot. Res.* **6**(2), 72–83 (1987).

https://doi.org/10.1017/S0263574711001032 Published online by Cambridge University Press

28. R. Kurtz and V. Hayward, "Multiple-goal kinematic optimization of a parallel spherical mechanism with actuator redundancy," *IEEE Trans. Robot. Autom.* **8**(5), 644–651 (1992).
29. O. Ma and J. Angeles, "Optimum Architecture Design of Platform Manipulator," **In**: *Proceedings of the IEEE International Conference on Robotics and Automation*, Nice, France (May 1991) pp. 1131–1135.
30. K. E. Zanganeh and J. Angeles, "Kinematic isotropy and the optimum design of parallel manipulators," *Int. J. Robot. Res.* **16**(2), 185–197 (1997).
31. D. Chablat, P. Wenger, F. Majoux and J.-P. Merlet, "An interval analysis based study for the design and the comparison of 3-DOF parallel kinematic machines," *Int. J. Robot. Res.* **23**(6), 615–624 (2004).
32. K. Julius, S. Steve, J. Allington, J.-E. Bobrow and D.-J. Reinkensmeyer, "Optimization of a parallel shoulder mechanism to achieve a high-force, low-mass, robotic-arm exoskeleton," *IEEE Trans. Robot.* **26**(4), 710–715 (2010).
33. G. Pritschow, K. -H. Wurst "Systematic design of hexapods and other parallel link systems," *Ann. CIRP* **46**(1), 291–295 (1997).
34. O. Company and F. Pierrot, "Modelling and design issues of a 3-axis parallel machine-tools," *Mech. Mach. Theory* **37**, 1325–1345 (2002).
35. T. Huang, D. J. Whitehouse and W. Jinsong, "The local dexterity, optimal architecture and design criteria of parallel machine tools," *Ann. CIRP* **47**(1) (1998).
36. J. Angeles, *Fundamentals of Robotic Mechanical Systems: Theory, Methods, and Algorithms*, 2nd ed. (Springer-Verlag, Heidelberg, Germany, 2003).
37. A. B. Koteswara, P. V. M. Rao and K. Saha, "Workspace and Dexterity Analyses of Hexaslide Machine Tools," *Proceedings of the IEEE International Conference on Robotics and Automation*, Taipei, Taiwan (Sep. 14–19, 2003).
38. J. Wang, C. Wu and X.-J. Liu, "Performance evaluation of parallel manipulators: Motion/force transmissibility and its index," *Mech. Mach. Theory* **45**(10), 1462–1476 (2010)
39. F. L. Lewis, C. T. Abdallah and D. M. Dawson, *Control of Robot Manipulators* (Macmillan, New York, 1993).
40. A. Codourey, "Dynamic modeling of parallel robots for computed-torque control implementation," *Int. J. Robot. Res.* **17**(2), 1325–1336 (1998).
41. J. Wu, W. Jinsong, L. Tiemin, L. Wang and L. Guan, "Dynamic dexterity of a planar 2-DOF parallel manipulator in a hybrid machine tool," *Robotica* **26**, 93–98 (2008).
42. L. Yunjiang, "Optimal Design of Parallel Manipulators," *Ph.D. Thesis* (Hong Kong University of Science and Technology, Hong Kong, 2006).
43. K. Deb, S. Agrawal, A. Pratap and T. Meyarivan, "A fast and elitist multiobjective genetic algorithm: NSGA-II," *IEEE Trans. Evol. Comput.* **6**(2), 182–197 (2002).
44. E. Zitzler, M. Laumanns and L. Thiele, "Spea2: Improving the Strength Pareto Evolutionary Algorithm," *Technical Report 103* (Computer Engineering and Networks Laboratory (TIK), ETH Zurich, Switzerland, 2001).

https://doi.org/10.1017/S0263574711001032 Published online by Cambridge University Press